

# Host traits and evolution shape key coral-bacterial symbioses

Francesco Ricci (✉ [riccif@student.unimelb.edu.au](mailto:riccif@student.unimelb.edu.au))

University of Melbourne

Kshitij Tandon

Biodiversity Research Center, Academia Sinica <https://orcid.org/0000-0003-3022-0808>

Jay Black

University of Melbourne

Kim-Ahn Lê Cao

University of Melbourne

Linda Blackall

University of Melbourne

Heroen Verbruggen

University of Melbourne

---

## Article

**Keywords:** Tropical Scleractinian Corals, Coral Microbiome, Holobiont, Microbial Reservoir

**Posted Date:** July 29th, 2021

**DOI:** <https://doi.org/10.21203/rs.3.rs-757354/v1>

**License:**  This work is licensed under a Creative Commons Attribution 4.0 International License.

[Read Full License](#)

---

# Host traits and evolution shape key coral-bacterial symbioses

Francesco Ricci<sup>a</sup>, Kshitij Tandon<sup>a,b</sup>, Jay R. Black<sup>c</sup>, Kim-Anh Lê Cao<sup>d</sup>, Linda L. Blackall<sup>a</sup>,

Heroen Verbruggen<sup>a</sup>

<sup>a</sup>School of BioSciences, University of Melbourne, Victoria, 3010, Australia

<sup>b</sup>Biodiversity Research Center, Academia Sinica, Taipei, 11529, Taiwan

<sup>c</sup>School of Geography, Earth and Atmospheric Sciences, University of Melbourne, Victoria, 3010,

Australia

<sup>d</sup>Melbourne Integrative Genomics, School of Mathematics and Statistics, University of Melbourne,

Victoria, 3010, Australia

## **Abstract**

The success of tropical scleractinian corals depends on their ability to establish symbioses with microbial partners. Host traits and evolution are known to shape the coral microbiome, but to what extent they affect its composition remains unclear. Here, by using twelve coral species representing the complex and robust clades, we show that functional traits and host evolutionary history explain 14% of the tissue and 13% of the skeletal microbiome composition, providing evidence that these predictors contribute to shaping the holobiont in terms of the presence and abundance of key bacterial species. Additionally, our study shows that the coral tissue and skeleton are dominated by rare bacteria and the skeleton can function as a microbial reservoir. Together, we provide novel insights into the processes driving coral-bacterial symbioses along with an improved understanding of the scleractinian tissue and skeleton microbiome.

21

22

23

## 24 **Introduction**

25 Ecology and evolution shape trait variation across species and populations, influencing host-  
26 microbiome associations (Freckleton and Jetz 2009; Bosch and McFall-Ngai 2011). Some of these  
27 relationships affect the fitness of the holobiont (Rosenberg et al. 2009), leading to remarkable  
28 evolutionary outcomes that have shaped life on Earth. Corals form a holobiont with unicellular  
29 microalgae (Symbiodiniaceae) and a diverse range of microbial communities. The coral holobiont is  
30 considered to be an independent level of selection (Zilber-Rosenberg and Rosenberg 2008) but our  
31 knowledge of the key mechanisms driving host-symbiont assemblages is fragmentary. It has been  
32 observed that host evolutionary processes (Pollock et al. 2018), skeletal architecture (Marcelino et al.  
33 2013; Fordyce et al. 2021) and mode of reproduction (Bernasconi et al. 2019; Damjanovic et al. 2019;  
34 Epstein et al. 2019) contribute to microbiome composition alongside other factors like season,  
35 environment, host health and developmental stage (O'Brien et al. 2020). Although previous studies have  
36 built a firm foundation for our knowledge of coral-bacterial associations, disentangling the individual  
37 and combined effects of these factors is paramount to understanding microbial community assembly.

38 Closely related species can harbour microbiota that resembles each other, a pattern known as  
39 phyllosymbiosis (Lim and Bordenstein 2020), which has been shown for several terrestrial and marine  
40 host-microbe systems, including corals (Bouffaud et al. 2014; Pollock et al. 2018; Griffiths et al. 2019;  
41 O'Brien et al. 2020). Phyllosymbiosis can be driven by a range of mechanisms, among which microbial  
42 filtering moderated by evolving host traits, abiotic and biotic ecological interactions of the host, or co-  
43 phylogenetic relationship between the host and microbes (Franzeburg et al. 2013; Douglas and Werren  
44 2016). However, its impact on the coral and the fraction of the microbiome involved remains enigmatic.

45 Several coral traits can affect the microbiome more directly. Coral skeletal architecture differs  
46 among species, affecting the physicochemical properties of the colony (Ricci et al. 2019) and microbial  
47 biomass (Fordyce et al. 2021). For instance, light scattering is a function of skeletal density (Marcelino  
48 et al. 2013) that results in different spatial gradients of light intensity and spectral composition that  
49 affect the microbiome (Magnusson et al. 2007; Ralph et al. 2007; Marcelino et al. 2013; Ricci et al.  
50 2021). Coral reproductive traits can influence the early microbiome, which plays key roles during coral

51 ontogeny and affects the fitness of the host (Damjanovic et al. 2019) and while broadcast spawning  
52 corals depend mostly on horizontal transmission (Lesser et al. 2013; Nitschke et al. 2016; Epstein et al.  
53 2019), brooding species exhibit some degree of vertical transmission (Quigley et al. 2018). Alongside  
54 reproductive mode and skeletal architecture, a range of host ecological and morphological traits are  
55 likely to take part in the establishment and development of the coral microbiome. For instance,  
56 interactions between planulae and crustose coralline algae were identified as potential cues influencing  
57 coral settlement (Jorissen et al. 2021) and the substrate of attachment is known to influence the  
58 holobiont (Massé et al. 2018). But whether coral bacterial communities can be predicted based on host  
59 traits is still to be investigated.

60         The coral microbiome is a dynamic system and an excellent case study of a highly diverse  
61 biological community contributing to holobiont success. Unravelling the composition of coral  
62 microbiomes is a necessary step towards understanding the interspecies relationships and functioning  
63 of the holobiont. The goal of our study was to disentangle the influence of drivers affecting the  
64 microbiome composition, with a particular focus on reproductive mode and coral skeletal traits as well  
65 as host evolutionary biology. Our experiment was also designed to reduce the variability introduced by  
66 a range of factors known to affect the coral holobiont, such as colony age (Williams et al. 2015), spatial-  
67 temporal variability (Dunphy et al. 2019) and health status (Maher et al. 2019).

## 68 **Results**

### 69 Experimental design

70 We sampled 12 coral species from the complex and robust clades aiming to disentangle differences in  
71 microbiome composition between host anatomical compartments and surrounding environment and to  
72 quantify to which extent host phylogeny, skeletal architecture and reproductive mode are associated  
73 with microbiome composition. Our sampling design also aimed to reduce factors known to affect the  
74 coral holobiont. We sampled only adult healthy colonies from a small geographic area, within three  
75 weeks and we characterized their tissue and skeletal prokaryotic communities using 16S rRNA  
76 amplicon sequencing. In order to disentangle the influence of host phylogeny, skeletal architecture and

77 reproductive mode on the bacteria residing in the tissue and skeleton (Fig. 1), we performed variation  
78 partitioning and canonical correspondence analysis (CCA). Then, we investigated and compared the  
79 microbial communities of the coral tissue and skeleton (Fig. 2), as well as surrounding seawater and  
80 sediment and assessed differences among groups using multivariate analyses and ordination.

### 81 Host traits and evolution shape the bacterial community composition

82 We quantified the influence of some of the most significant processes known to take part in the  
83 establishment and development of the coral microbiome, like host phylogeny (Pollock et al. 2018),  
84 skeletal architecture (Fordyce et al. 2021) and reproductive mode (Damjanovic et al. 2019; Epstein et  
85 al. 2019), by applying variation partitioning analysis to the tissue and skeletal bacterial communities.  
86 Our models explained 14% of the tissue and 13% of the skeletal microbiome variation, leaving a high  
87 proportion of the variation (>85%) unexplained by the predictors (Fig. 3). This is not fully surprising  
88 since past reports have found that the coral microbiome is variable within a single coral colony  
89 (Damjanovic et al. 2020), among individuals, species and reef habitat (Ainsworth et al. 2015; Hester et  
90 al. 2016; Hernandez-Agreda et al. 2016). We argue that a combination of unmeasured environmental  
91 variables, functional redundancy, community assembly processes and physicochemical properties  
92 specific to each coral colony likely take part in determining the coral holobiont assemblage and limiting  
93 its broader consistency.

### 94 *Host evolution drives key coral bacterial associations*

95 Employing LeFSe analysis, we identified members of the coral microbiome that preferentially  
96 colonized the coral tissue or skeleton (Supp. Data 1; Supp. Fig. 1), then through CCA analysis we  
97 assessed their association with host phylogenetic history and coral traits. In the CCA analysis the three  
98 coral phylogenetic variables (PV1, PV2 and PV3 - see Host phylogeny in M&M) showed a strong  
99 association with some ASVs (Fig. 4a and 4b).

100 *Endozoicomonas* preferentially colonized the coral tissue (Supp. Fig. 1) and individual ASVs  
101 belonging to this genus were associated with corals in the robust clade (Fig. 4a; positive correlation  
102 with phylogenetic variable PV1) and the families Poritidae (Fig. 4a) positive correlation with

103 phylogenetic variable PV2) and Pocilloporidae (Fig. 4a; positive correlation with phylogenetic variable  
104 PV3). Our results confirmed *Endozoicomonas* being a highly prevalent coral symbiont across coral  
105 species (Neave et al. 2017; Tandon et al. 2020) and are also in agreement with Pollock et al. (2018),  
106 who proposed phyllosymbiosis between this bacterial group and corals. Although the knowledge about  
107 the processes driving phyllosymbiosis is still fragmentary, evidence shows that host-filtering may play  
108 a role (Mazel et al. 2018). By assessing patterns of association of entire microbiomes with their hosts,  
109 phyllosymbiosis also takes into account some long-term host-microbe relationships that have developed  
110 into symbioses (O'Brien et al. 2020) and, because of *Endozoicomonas* putative beneficial roles like  
111 nutrients provision and aiding host homeostasis (Neave et al. 2016; Tandon et al. 2020), it seems likely  
112 that these bacteria developed a mutualistic symbiosis with corals over time.

113 *Alteromonas* and *Pseudoalteromonas* preferentially colonized the tissue of robust corals and in  
114 the family Pocilloporidae (Fig. 4a; Supp. Fig. 1). Additionally, *Pseudoalteromonas* was associated with  
115 the family Poritidae (Fig. 4a). This is the first evidence of phyllosymbiosis between these coral lineages  
116 and bacterial genera thought to take part in nitrogen cycling and antibacterial activity in the coral  
117 holobiont (Shnit-Orland et al. 2012; Ceh et al. 2013a).

118 Bacteria in the genera *Spirochaeta* and “*Candidatus Amoebophilus*” preferentially colonized  
119 the coral skeleton (Supp. Fig. 1) and individual ASVs belonging to these genera were associated with  
120 corals in the robust clade and the family Poritidae (Fig. 4b), in line with the results of Pollock et al.  
121 (2018). Our data also indicate phyllosymbiosis for *Spirochaeta*, bacteria that usually thrive in oxygen  
122 deprived environments (Leschine et al. 2006) like the coral skeleton and could be pivotal members of  
123 the coral holobiont because of their ability to fix nitrogen and carbon (Lawler et al. 2016). Despite  
124 “*Candidatus Amoebophilus*” having been flagged as a member of the coral core microbiome  
125 (Ainsworth et al. 2015; Ricci et al. 2021), its role in the holobiont is still unclear. Available data on  
126 “*Candidatus Amoebophilus*” (Kantor et al. 2015) and “*Candidatus Amoebophilus asiaticus*” (Schmitz-  
127 Esser et al. 2010) show reduced genomes with limited metabolic capabilities, suggesting they may rely  
128 on the host for survival. Interestingly, “*Candidatus Amoebophilus asiaticus*” genome harbours a high  
129 count of host cell interaction genes, particularly a wide arsenal of eukaryotic domain-like proteins.

130 These proteins are used by intracellular pathogens to interact with hosts and modulate host response via  
131 multitude protein-protein interactions (Schmitz-Esser et al. 2010).

132 Bacteria in the Myxococcales order preferentially colonized the coral skeleton (Supp. Fig. 1)  
133 and were associated with corals in the robust clade (Fig. 4b). Moreover, recent studies have shown that  
134 these microbes might have co-diversified with corals (Pollock et al. 2018). Myxococcales are known to  
135 play beneficial roles in other systems like agricultural settings (Wang et al. 2020a), where they keep  
136 pathogen populations under control by releasing large quantities of antibiotics. The skeleton of many  
137 corals analyzed in this study concurrently harboured high abundance of Myxococcales and potential  
138 pathogenic bacteria (*i.e. Vibrio* and *Serratia*). Thus, as reported for agricultural settings and given that  
139 all the sampled colonies were visibly healthy, the Myxococcales may play similar roles in the coral  
140 holobiont by controlling pathogen populations (Rosales et al. 2019).

#### 141 *Skeletal architecture affects the microbial abundance*

142 Skeletal architecture influenced the composition of tissue and skeletal microbiomes (Fig. 3). The  
143 skeleton affects the physicochemical properties of the whole coral colony including the tissue and  
144 Marcelino et al. (2013) found that, by refracting light back, the skeleton alters the light environment in  
145 the tissue, affecting the Symbiodinaceae. One could argue that this also causes downstream effects on  
146 other members of the tissue microbiome. Accordingly, we found that skeletal architecture was  
147 associated with several key members of the tissue microbiome, including *Endozoicomonas*,  
148 *Alteromonas* and *Pseudoalteromonas* (Fig. 4a). Our results also indicate that skeletal architecture alters  
149 the abundance of bacterial species rather than filtering them out entirely. For instance, we found that  
150 despite the bacterial genera *Bacillus*, *Halomonas*, *Pseudoalteromonas* and *Vibrio* being mainly  
151 associated with corals with porous skeletons like *A. aspera* and *M. digitata*, they were also present in  
152 species with denser skeletons at low abundance. Similarly, the bacterial families Kiloniellaceae and  
153 Hyphomonadaceae, as well as the genus *Rugeria* that we found at higher abundance in species with  
154 denser skeletons (e.g. *P. sinensis*, *G. retiformis*), were also present in corals with more porous skeletons  
155 at low abundance.

156 *Reproductive mode promotes beneficial functional associations*

157 Our data show that tissue and skeletal microbiomes of scleractinian corals were influenced by the  
158 reproductive mode (Fig. 3) and the reproductive mode variables (broadcast spawners, brooders and  
159 mixed mode) were associated with key holobiont members, including *Endozoicomonas*, *Alteromonas*,  
160 *Pseudoalteromonas* and Myxococcales (Fig. 4a and 4b). These bacteria are all known for their  
161 beneficial roles (Shnit-Orland et al. 2012; Ceh et al. 2013a; Neave et al. 2016; Rosales et al. 2019) and  
162 possibly benefiting early developmental stages of the coral through nutrient cycling and facilitating  
163 early immune system development. But, in the tissue, reproductive mode was also associated with  
164 controversial bacteria like *Serratia* and *Vibrio* (Fig. 4a), which are known as potential pathogens in  
165 some coral species (Ben-Haim et al. 2002; Alagely et al. 2011; Bernasconi et al. 2019). We argue that  
166 these putative pathogens, in normal conditions, are commensal members of the holobiont, while as  
167 suggested in previous studies their detrimental potential could emerge during dysbiotic states (Kemp et  
168 al. 2018).

169 Variation partitioning analysis showed that reproductive mode explained a portion of the  
170 microbiome variation (tissue: 3% and skeleton: 4%; Fig. 3). Studies investigating the establishment of  
171 microbiomes reported that corals can vertically transmit a consortium of bacteria (Leite et al. 2017;  
172 Zhou et al. 2017; Damjanovic et al. 2019; Bernasconi et al. 2019; Epstein et al. 2019). Similarly, our  
173 CCA analysis showed that some bacterial groups highlighted by these studies (*i.e.* *Acinetobacter* spp.,  
174 *Bacillus* spp., Caulobacterales, Cryomorphaceae, Endozoicomonadaceae, *Pseudomonas* spp.,  
175 Rhizobiales, Rhodobacterales) were likely vertically transmitted in the species analyzed in our study.  
176 The correspondence between our findings and past reports shows that coral reproductive mode  
177 influences the microbiome composition predictably and that early host-symbiont associations persist  
178 across a coral's lifetime.

179 Besides the microbial taxa reported to be vertically inherited in corals before, our results show  
180 that reproductive mode correlated with a range of other bacteria, suggesting they may also get  
181 transferred from parents to offspring and, based on their roles in other systems, they can be hypothesized  
182 to play roles in host development as well. Among the genera we found to be associated with the

183 reproductive modes mixed and brooders, *Stenotrophomonas* are known to cycle sulfur and nitrogen  
184 compounds in plants (Ryan et al. 2009) and *Massilia* are known to stimulate plant growth by producing  
185 compounds like siderophores (Ofek et al. 2012). Nutrient cycling and pathogen control seem to be two  
186 common functional features among vertically transmitted bacteria, increasing survival rate and fitness  
187 of developing corals (Ceh et al. 2013b; Zhou et al. 2017). Thus, by influencing the early microbiome,  
188 the reproductive mode could drive host-bacteria functional associations pivotal during coral ontogeny.

### 189 Coral microbiomes are dominated by rare species

190 Except for a few bacteria that were consistently present across several coral species, rare species  
191 dominated the coral microbiomes. The great majority of bacterial ASVs (99.6% for tissue and 99.7%  
192 for skeleton) were not consistently present in at least 30% of the samples. The core microbiome, i.e. the  
193 ASVs occurring in at least 30% of samples, consisted of only 14 ASVs in the tissue and 9 in the skeleton  
194 (Supp. Data 2).

195 A closer look at microbiome variability within species showed that even within closely related  
196 hosts most bacterial ASVs were rare, leading to wide variability between samples. The skeletal microbiome  
197 showed a higher proportion of core members than the tissue microbiome for 8 out of 12 coral species  
198 (Supp. Data 3). Since the microbial communities of tissue and skeleton were dominated by rare bacterial  
199 ASVs, we analyzed their Pielou's evenness, a measure indicating how similar the abundances of  
200 different species in the microbiome are (Jost 2010). Despite finding comparable evenness of the tissue  
201 and skeletal bacterial communities (Supp. Fig. 2a), when we compared across coral species we found  
202 high variability in the evenness of both tissue and skeletal microbiome (Supp. Fig. 2b and 2c). For  
203 instance, in *G. retiformis* both tissue and skeletal microbiomes showed evenly distributed bacterial  
204 populations, while in *P. australensis* the tissue microbiome was dominated by the genus  
205 *Endozoicomonas* and the families Caldicoprobacteraceae, Thermoanaerobaculaceae and  
206 Cyclobacteriaceae dominated the skeletal microbiome of individual samples. In line with our results,  
207 it has been previously reported that the microbiome composition of each coral species can show various  
208 degrees of diversity (McDevitt-Irwin et al. 2017) and in some cases one or a few bacterial taxa can be  
209 dominant, like in *P. verrucosa*, whose bacterial community is dominated by the genus *Endozoicomonas*

210 (Voolstra and Ziegler 2020). A range of processes including host evolution (Pollock et al. 2018), traits  
211 (Damjanovic et al. 2019; Epstein et al. 2019), microniches partitioning (Ricci et al. 2019), priority  
212 effects and functional redundancy (Louca et al. 2016) may synergistically affect the microbiome  
213 assembly and ultimately determine the variability of corals' bacterial communities.

214         Rare bacteria are understudied in many environments, but it is known that their presence and  
215 abundance are often driven by environmental variables (Campbell et al. 2011) and this is probably true  
216 for the coral holobiont too. Voolstra and Ziegler (2020) suggested that functional redundancy may  
217 promote high microbiome flexibility and we argue that this process may also structure the rare portion  
218 of the coral microbiome. Although our study design is not geared towards investigating whether the  
219 coral microbiome is driven by functional redundancy, our analysis of rare bacteria (observed in <50  
220 reads per sample) that are likely involved in nitrogen and sulfur metabolism suggest that coral samples  
221 often featured unique ASVs of these guilds (Supp. Data 4), e.g. nitrogen fixers in the Rhizobiales (Wang  
222 et al. 2020b) or sulfate reducers in the Deltaproteobacteria and Thermodesulfobacteria (Henry et al.  
223 1994; Chen et al. 2021). While these data alone do not prove that functional redundancy is at the basis  
224 of the observation that a large proportion of bacterial ASVs in the coral microbiome is very rare, they  
225 do suggest that at least in some cases rare bacteria fill functional niches in the coral holobiont.

#### 226 Coral tissue and skeletal microbiomes overlap but differ quantitatively

227         Our results are in clear agreement with the hypothesis formulated by Marcelino et al. (2017)  
228 that the skeleton can serve as a reservoir for coral tissue microbes. Indeed, our work shows that a large  
229 fraction of bacteria can colonize both anatomical compartments (*i.e.* 86% of tissue ASVs were found  
230 in at least one skeleton sample and 56% of skeletal ASVs were found in at least one tissue sample). On  
231 the basis of this, it can be argued that after a period of dysbiosis, beneficial bacteria could quickly  
232 repopulate the tissue from the skeleton (Marcelino et al. 2017). Despite this, the  $\beta$ -diversity of coral  
233 tissue and skeletal microbiomes differed significantly for all coral species ( $p$  values in range 0.006 -  
234 0.019) except *P. daedalea* (Supp. Fig. 3). Therefore, our results indicate that while many bacteria are  
235 not selective in colonizing the coral tissue or skeleton, the complex array of biotic and abiotic

236 interactions characteristic of each compartment shapes its microbiome composition differently (Fig. 5;  
237 Supp. Fig. 3).

238 Coral tissue and skeleton are also known to differ in their physicochemical environment, with  
239 the skeleton offering a wide array of microniches (Ricci et al. 2019) and one study has reported that the  
240 skeletal communities are more diverse than their tissue counterparts (Pollock et al. 2018). Our data  
241 showed comparable  $\alpha$ -diversities of tissue and skeleton microbiomes for most coral species (Supp. Fig.  
242 4). This conflicts with the findings of Pollock et al. (2018) and while it may represent an underlying  
243 biological cause, methodological differences between the studies may also contribute to the observed  
244 differences (e.g. using ASVs vs. OTUs for taxonomic resolution).

#### 245 Sourcing the microbiome: vertical and (or) horizontal acquisition

246 Our results suggest that both the tissue and skeleton have a component of vertically acquired bacteria,  
247 whereas it is likely that the remaining microbiome portion is more dynamic and taken up from the  
248 environment during different seasons and life stages of the host. Our comparison of the coral microbiota  
249 with those of the surrounding seawater and sediment showed that bacterial species shared between  
250 corals and their environment at the time of sampling accounted for more than 30% of the ASVs in *A.*  
251 *aspera* and *P. damicornis* (Supp. Data 5). In line with our results, recent studies show that the vertically  
252 and horizontally acquired microbiome varies among coral species (Leite et al. 2017; Zhou et al. 2017;  
253 Bernasconi et al. 2019; Epstein et al. 2019). For instance, in *P. damicornis* the bacterial community  
254 establishment is largely driven by the microbiome present in the environment (Epstein et al. 2019) while  
255 in *A. digitifera*, *A. gemmifera* and *Mussismilia hispida*, there is evidence of vertical transmission of a  
256 wider microbiome portion (Leite et al. 2017; Zhou et al. 2017; Bernasconi et al. 2019). Moreover,  
257 although for some coral species we found a low similarity between their microbiome and that of  
258 concurrently sampled seawater and sediment (Supp. Data 5), this by no means implies that  
259 environmental acquisition is not an influential process in the establishment of these coral species'  
260 microbiome. Given that our seawater and sediment samples were taken over a period of 1 month, it

261 seems likely that a more prolonged sampling would recover a higher fraction of the coral microbiome  
262 in these and other potential environmental reservoirs.

### 263 Unusual suspects show persistent associations with corals

264 Our work identified several bacteria that were consistently associated with corals but are either new to  
265 the coral microbiome field or understudied. Cyclobacteriaceae were present in at least one sample of  
266 eight coral species except for *A. aspera*, *G. tenuidens*, *I. palifera* and *S. pistillata*. Currently,  
267 Cyclobacteriaceae have only been reported in 7-months-old *Acropora* recruits (Chan et al. 2018) and  
268 their intra-colony changes in abundance after *Acropora* spp. bleaching (Durante et al. 2019). Our work  
269 shows that this family is much more widespread across the complex and robust clades. From a  
270 functional point of view, members of this family could benefit the coral through their metabolic  
271 capabilities including carbohydrate metabolism, carotenoid biosynthesis, antibiotic resistance and  
272 quorum-sensing regulation (Pinnaka and Tanuku 2014).

273 Bacteria in the genus *Paramaledivibacter* were found in six *P. lutea*, three *P. daedalea* and two  
274 *P. australensis* samples. To our knowledge, this is the first time for this genus of strictly anaerobic  
275 bacteria to be reported in the coral literature. While at this stage we can only guess as to its functions in  
276 the coral holobiont, it might be a harmful species due to its ability to degrade amino acids and peptides  
277 (Li et al. 2016). As mentioned above, detrimental effects by pathogens could be counterbalanced by  
278 beneficial holobiont members including Myxococcales and *Pseudoalteromonas*. Despite  
279 *Paramaledivibacter* being described as strictly anaerobic, we did find these bacteria in the coral tissue.  
280 This finding could sound surprising, but this is not the first study reporting obligate anaerobes in coral  
281 compartments known to show oxygen presence (Marcelino and Verbruggen 2016; Cai et al. 2017).

282 *Roseospira* has also not been reported in the coral literature before, but we found these bacteria  
283 in the tissue and skeleton of three *P. lutea*, two *G. retiformis*, one *G. tenuidens* and one *P. daedalea*  
284 samples. These purple non-sulfur bacteria seem to be able to colonize a diverse range of environments  
285 and optimally grow photoheterotrophically (Guyoneaud et al. 2002). Thus, given their ability of  
286 utilizing substrates known to be present in corals like acetate (Patton et al. 1977) and glutamate (Su et

287 al. 2018) and using near-infrared wavelengths not absorbed by Symbiodiniaceae, the coral colony could  
288 offer an array of microniches where these bacteria's niche preferences are met.

## 289 **Discussion**

290 Through a combination of a homogeneous experimental design that minimizes external biases affecting  
291 the microbiome, use of innovative technologies like micro-CT scanning to quantify host traits and the  
292 application of a range of statistical analyses, our study allowed us to unravel the structure of the coral  
293 microbiome and quantify how it is influenced by host traits and evolution.

294 We showed a significant association of host evolution and traits with the bacterial community,  
295 including a range of host-bacterial relationships known to affect holobiont health and functioning.  
296 Based on our results, we hypothesize that reproductive mode could aid vertical transmission of bacteria  
297 beneficial to corals' development, while skeletal architecture works like a filter affecting bacteria  
298 abundance. Although our analysis accounted for some of the most influential processes known to affect  
299 the microbiome composition, these could only marginally explain the microbiome variation of tissue  
300 and skeleton. A holistic view of the mechanisms determining the holobiont composition will be gained  
301 by incorporating the physicochemical and dynamic biochemical environment of the coral colony and  
302 its influence on the structure of the microbiome and also by assessing whether the presence of some  
303 bacteria (whether dominant or rare) may influence the overall structure of the microbiome. In this study,  
304 we provided substantial evidence that coral tissue and skeletal microbiomes are dominated by rare taxa  
305 and differ in compositions, but a consortium of bacteria can colonize both compartments and the  
306 skeleton could be a microbial reservoir.

307 While our study answers several unsolved questions about the bacterial community structure  
308 of scleractinian corals and the mechanisms driving its composition, it also exposes knowledge gaps.  
309 Despite our study's focus on commonly studied coral species, we identified several abundant bacterial  
310 groups that were not previously reported in coral literature. This highlights that the field of coral reef  
311 microbial ecology still presents substantial hiatuses even at the level of characterizing the taxonomic  
312 composition of the microbiome and substantial further work will be needed to fully characterize the

313 microbiome, understand its functions in the coral holobiont, its fine-scale distribution in relation to  
314 ecological micro-niches and the metabolic hand-offs that happen among microbiome members and with  
315 the host. The use of putative beneficial microorganisms has been proposed as a tool to mitigate the  
316 increasing pressure of anthropogenic activities on coral reefs (Peixoto et al. 2020), therefore we hope  
317 that the detailed knowledge about community structure gained in our study can form the basis for further  
318 advances in probiotic strategies to improve coral resilience in future climate scenarios.

## 319 **Material and Methods**

### 320 Sample collection, processing and statistics

321 All the samples were collected under the permit G19/41658.1 issued by the Great Barrier Reef Marine  
322 Park Authority. Seventy-two coral fragments (collected at low tide <1 water depth), five seawater  
323 samples (5 L each) and five 50 mL sediment samples were collected from the research zone of Heron  
324 Island reef flat, central Great Barrier Reef (GBR; 23°44'S, 151°91'E), during January 2020. Corals were  
325 collected using a sterile hammer and chisel and placed in sterile zip-lock polyethylene bags in seawater.  
326 Coral tissue was removed from the skeleton of each sample using a waterpik and sterile seawater (SSW),  
327 then tissue slurry and skeletal fragments were collected and snap-frozen by immersion in liquid nitrogen  
328 and stored at -80 °C until processing. The seawater samples and 2 samples of SSW (5 L each) were  
329 filtered using 0.22 µm filters (MilliporeSigma) before snap freezing. By sequencing the tissue and  
330 skeletal microbiome of 72 corals (144 samples in total) belonging to 12 species in the complex and  
331 robust clades, five seawater and sediment samples each, we retrieved 7,025,745 16S rRNA sequences  
332 (sample minimum: 2,073; mean: 46,528; maximum: 115,692). Because of the comparative nature of  
333 this study, we took a range of precautions to avoid any potential cross contamination and  
334 computationally removed potential contaminants. For instance, we sequenced SSW used to remove the  
335 coral tissue contaminants; sampled skeletal fragments 5 mm from the tissue to prevent tissue-skeleton  
336 microbiomes cross contaminations; and sequenced control samples taken during the DNA extraction  
337 and amplification.

338 Library preparation, sequencing and initial quality control

339 The total DNA of each coral tissue, coral skeleton, seawater, sediment and control sample was extracted  
340 using the Wizard Genomic DNA Purification Kit (Promega). Extractions were also performed on eight  
341 blanks taken during both the extraction and amplification protocols. SSW and blanks served as controls.  
342 We used a 2-step PCR amplification, the first amplifying the target marker and the second adding  
343 Illumina adapters (underlined). The V5-V6 regions of the 16S rRNA were PCR amplified using the  
344 primer pairs: 784F [5'-  
345 TCGTCGGCAGCGTCAGATGTGTATAAGAGACAGAGGATTAGATACCCTGGTA -3'] and  
346 1061R [5'- GTCTCGTGGGCTCGGAGATGTGTATAAGAGACAGCRRACGAGCTGACGAC -  
347 3'] (Andersson et al. 2008).

348 Sequences were processed using the QIIME2 pipeline version 2020.11 (Bolyen et al. 2018).  
349 Cutadapt was used to remove primers (Martin 2011). DADA2 was used to merge forward and reverse  
350 reads, remove poor-quality sequences, perform dereplication and eliminate chimeras (Callahan et al.  
351 2016). Taxonomy was assigned using the feature-classifier plugin in-built in QIIME2 - SILVA v128  
352 QIIME release (Quast et al. 2012).

353 Host phylogeny

354 We confirmed the identity of the targeted corals based on skeletal morphology. The phylogeny of the  
355 12 coral species was extracted from the multigene molecular phylogeny of corals published by Huang  
356 and Roy (2015). We took their set of supertrees and derived a consensus tree in TreeAnnotator (BEAST  
357 2.4.8; Bouckaert et al. 2019). We computed a matrix of pairwise patristic distances from the  
358 phylogenetic tree with the distTips function from adePhylo (Jombart and Dray 2010) and performed  
359 non-metric multidimensional scaling (NMDS, isoMDS from MASS; Venables and Ripley 2002) to  
360 obtain a set of variables that can be used to relate the host phylogeny to the microbiome in multivariate  
361 analyses. The vectors of the positions of the coral species along the three dimensions of the NMDS  
362 were used to represent host phylogeny in downstream analyses dividing it into three main phylogenetic  
363 variables. Phylogenetic variable PV1 separated the robust from the complex corals, the robust clade  
364 positively correlating with PV1 (*Goniastrea retiformis*, *Paragoniastrea australensis*, *Platygyra*

365 *daedalea*, *Platygyra sinensis*, *Pocillopora damicornis* and *Stylophora pistillata*) and negatively with  
366 the complex clade (*Acropora aspera*, *Goniopora tenuidens*, *Isopora palifera*, *Montipora digitata*,  
367 *Porites annae* and *Porites lutea*). Phylogenetic variable PV2 represents the phylogenetic subdivision  
368 of complex species into Poritidae (*G. tenuidens*, *P. lutea* and *P. annae*), which correlated positively  
369 with PV2 and the Acroporidae (*A. aspera*, *I. palifera* and *M. digitata*), which correlated negatively with  
370 PV2. Phylogenetic variable PV3 represents the phylogenetic subdivision of the robust species into  
371 Pocilloporidae (*P. damicornis* and *S. pistillata*) that correlated positively with PV3 and the Faviidae  
372 (*G. retiformis*, *P. australensis*, *P. daedalea* and *P. sinensis*) that correlated negatively with PV3.

### 373 Skeletal architecture

374 Portions of all 72 coral fragments were scanned using a Phoenix Nanotom M micro-CT scanner  
375 (Waygate Technologies) capturing the full specimen structure at a voxel resolution of 20  $\mu\text{m}$ . Further  
376 to this, a 12 mm x12 mm x12 mm region-of-interest (ROI) from one sample of each of the 12 species  
377 were scanned at a 10  $\mu\text{m}$  resolution. Preserved samples were scanned in air and secured within a  
378 specimen jar with bubble wrap to prevent movement during scanning. Scans were collected using the  
379 datos|x acquisition software (Waygate Technologies) and X-ray energy of 110kV and 300 mA with a  
380 tungsten target and 0.1 mm copper filter to pre-harden the X-ray beam. A fast scan setting was used  
381 collecting between 1199 to 1798 projections through a full 360° rotation of the specimens, depending  
382 upon sample width on the instrument detector, with an integration time of 0.5 seconds per projection  
383 leading to a 10 to 15 minute scan time. Large specimens were scanned twice to capture the full specimen  
384 structure using a multiscan feature.

385 Micro-CT data was reconstructed using the datos|x reconstruction software (Waygate  
386 Technologies) applying an ROI and inline median filter during the reconstruction of the data.  
387 Reconstructed data was imported into Avizo version 2019.3 (Thermo Scientific) for analysis. The  
388 structure of each coral specimen was evaluated by segmenting three different phases observed in scans,  
389 the dense skeletal phase (bright white structure in Supp. Fig. 5a), a lower density organic phase  
390 (intermediate gray values in Supp. Fig. 5a) and trapped air within the structure phase (dark gray-black  
391 space in Supp. Fig. 5a). The Auto Threshold algorithm of Avizo was used for segmentation of the 3

392 phases (Supp. Fig. 5b), which is based on a factorization method developed by Otsu (1979) and  
393 determines the point for segmentation between phases in the grayscale histogram (Supp. Fig. 5c). To  
394 determine the total porosity ( $V_{\text{porosity}}$ , Eq. 1a) of specimens a sample mask was created by using the  
395 Closing and Fill Holes operations of Avizo on the segmented skeleton ( $V_{\text{skeleton}}$ , Eq. 1a) plus organic  
396 matter ( $V_{\text{organic}}$ , Eq. 1a) to produce a solid sample mask ( $V_{\text{sample}}$ , Eq. 1a) encompassing the boundaries  
397 of the sample. The total volume of segmented air ( $V_{\text{pores}}$ , Eq. 1b) and organic phase ( $V_{\text{organic}}$ , Eq. 1b)  
398 within the sample mask is then taken as a measure of sample porosity (Eq. 1b). Segmented label  
399 volumes were calculated using the Volume Fraction algorithm in Avizo, which also determines the  
400 volume fraction of each phase relative to the segmented sample mask. To determine whether the 20  
401 micrometer resolution scan sufficiently captured micro-porosity within the skeleton the 10 micrometer  
402 scans were registered to the 20 micrometers scans using the Register Images algorithm of Avizo. The  
403 same 12x12x12 mm<sup>3</sup> ROI was then extracted from the 20 micrometer dataset and trends in porosity  
404 compared between the two datasets at different resolutions (Supp. Fig. 5).

405

$$406 \quad V_{\text{sample}} = V_{\text{skeleton}} + V_{\text{porosity}} \quad (1a)$$

$$407 \quad V_{\text{porosity}} = V_{\text{organic}} + V_{\text{pores}} \quad (1b)$$

408

409 Bulk skeletal density (dry weight of the skeleton /  $V_{\text{sample}}$ ; g/cm<sup>3</sup>) and porosity ( $V_{\text{porosity}} / V_{\text{sample}} \times 100$ ; %)  
410 were the two main parameters we derived from downstream analysis of the skeletal  
411 architecture dataset. These two parameters are strictly correlated with each other, indeed, as porosity  
412 decreases, bulk skeletal density approaches micro-density and neither can exceed the density of pure  
413 aragonite (2.94 mg mm<sup>-3</sup>; Caroselli et al. 2016). The complementarity of the two parameters also has  
414 implications on the analytical procedure used to measure them, resulting in multicollinearity in  
415 downstream analyses. Therefore, we decided to only retain the parameter porosity as representative of  
416 skeletal architecture.

#### 417 Reproductive mode

418 The reproductive mode of each coral species was retrieved from Coral Trait Database (CTDB) v. 1.1.1  
419 (<https://coraltraits.org/>; Madin et al. 2016) and we divided them into three groups: broadcast spawners  
420 (*A. aspera*, *G. retiformis*, *G. tenuidens*, *M. digitata*, *P. annae*, *P. australensis*, *P. daedalea*, *P. lutea*, *P.*  
421 *sinensis*), brooders (*I. palifera*, *S. pistillata*) and mixed (*P. damicornis*).

#### 422 Statistical analysis

423 The significance level for statistical analyses was 0.05 and unless stated otherwise all analyses were  
424 conducted on rarefied ASVs tables (10,000 sequences per sample). Differences in community  
425 composition ( $\beta$ -diversity) among coral skeleton, tissue, seawater and sediment microbiomes were  
426 computed using center log-transformed Euclidean distance matrices of the rarefied ASV tables.  
427 Differences among groups were tested using non-parametric multivariate analysis of variance  
428 (NPMANOVA), Linear discriminant analysis Effect Size (LEfSe; Segata et al. 2011) and visualized  
429 with principal component analysis (PCA). LEfSe implemented in *microbiomeMarker* (Yang Cao 2020)  
430 was used to identify differentially abundant ASVs among groups by coupling statistical tests to assess  
431 their differences with further tests encoding biological consistency and effect relevance. ASVs with  
432  $\log(\text{LDA}) > 3$  (Kruskal-Wallis test:  $p < 0.05$ ) were considered differentially abundant. Z-score  
433 transformed abundance profiles of LEfSe identified ASVs were visualized using heatmap via *heatmap*  
434 (Kolde 2012). Associations between the microbiome and predictor variables (host phylogeny, skeletal  
435 architecture and reproductive mode) were assessed via variation partitioning analysis (Legendre et al.  
436 2005) and canonical correspondence analysis (CCA; Ter Braak 1987), using Hellinger transformed,  
437 rarefied ASV tables. CCA is a multivariate method that can disentangle patterns or changes in biological  
438 communities and identify potential associations between explanatory variables and ASVs (based on  
439 their coordinates' similarity on the CCA plots). Both analyses (variation partitioning and CCA) were  
440 performed on the top 200 most abundant ASVs of the dataset, both to reduce its dimension and because  
441 rare species may have an unduly large influence on these types of analysis (Legendre and Gallagher  
442 2001). All analyses were conducted using RStudio version 1.2.5033 and packages *agricolae* (de  
443 Mendiburu and Yaseen 2020), *ampvis2* (Andersen et al. 2018), *ape* (Paradis and Schliep 2019),

444 *decontam* (Davis et al. 2018), *dplyr* (Wickham 2015), *ggfortify* (Tang et al. 2016), *ggplot2* (Wickham  
445 2011), *ggvegan* (Simpson 2015), *microbiome* (Lahti and Shetty 2018), *microbiomeMarker* (Yang Cao  
446 2020), *phreatmap* v1.0.12 (Kolde 2012), *phyloseq* (McMurdie and Holmes 2013), *rgr* (Garrett 2013)  
447 and *vegan* (Simpson 2015).

448

#### 449 **Acknowledgments**

450 We thank the staff at Heron Island Research Station for providing assistance and Stephen Wilcox from  
451 the Walter and Eliza Hall Institute for supervising the molecular analysis and facilitating sequencing.  
452 We acknowledge the Melbourne TrACEES Platform (Trace Analysis for Chemical, Earth and  
453 Environmental Sciences) for access to the micro-CT scanner. KT is thankful to Dr. Sen-Lin Tang from  
454 Biodiversity Research Center, Academia Sinica, Taiwan for hosting him in his laboratory. We  
455 acknowledge funding from the Australian Research Council (DP200101613 to HV and LLB), the  
456 National Health and Medical Research Council (NHMRC) Career Development fellowship  
457 (GNT1159458) to KALC, the Environmental Microbiology Research Initiative at the University of  
458 Melbourne (to FR), the Native Australian Animal Trust (to FR) and the Holsworth Wildlife Research  
459 Endowment (to FR).

#### 460 **Data availability**

461 Sequence data determined in this study are available at NCBI under SRA Accession PRJNA719930  
462 (<https://www.ncbi.nlm.nih.gov/sra/PRJNA719930>).

463

#### 464 **Supplementary Material**

465 Supplementary data, data analysis workflow, raw tables, high quality figures and plots are available at  
466 <https://figshare.com/search?q=Host+traits+and+evolution+shape+key+coral-bacterial+symbioses>

#### 467 **Conflict of interest**

468 On behalf of all authors, the corresponding author states that there is no conflict of interest.

469 **References**

- 470 Ainsworth TD, Krause L, Bridge T, Torda G, Raina JB, Zakrzewski M, Gates RD, Padilla-Gamino JL, Spalding  
471 HL, Smith C, Woolsey ES, Bourne DG, Bongaerts P, Hoegh-Guldberg O, Leggat W (2015) The coral core  
472 microbiome identifies rare bacterial taxa as ubiquitous endosymbionts. *The ISME Journal* 9:2261-2274
- 473 Alagely A, Krediet CJ, Ritchie KB, Teplitski M (2011) Signaling-mediated cross-talk modulates swarming and  
474 biofilm formation in a coral pathogen *Serratia marcescens*. *The ISME journal* 10:1609-20.
- 475 Andersen KS, Kirkegaard RH, Karst SM, Albertsen M (2018) ampvis2: an R package to analyse and visualise  
476 16S rRNA amplicon data. *BioRxiv:299537*
- 477 Andersson AF, Lindberg M, Jakobsson H, Bäckhed F, Nyrén P, Engstrand L (2008) Comparative analysis of  
478 human gut microbiota by barcoded pyrosequencing. *PloS one* 3:e2836
- 479 Ben-Haim Y, Rosenberg E (2002) A novel *Vibrio* sp. pathogen of the coral *Pocillopora damicornis*. *Marine*  
480 *Biology* 1:47-55
- 481 Bernasconi R, Stat M, Koenders A, Paparini A, Bunce M, Huggett MJ (2019) Establishment of coral-bacteria  
482 symbioses reveal changes in the core bacterial community with host ontogeny. *Frontiers in microbiolog*  
483 *10:1529*
- 484 Bolyen E, Rideout JR, Dillon MR, Bokulich NA, Abnet C, Al-Ghalith GA, Alexander H, Alm EJ, Arumugam M,  
485 Asnicar F (2018) QIIME 2: Reproducible, interactive, scalable and extensible microbiome data science.  
486 *PeerJ Preprints*
- 487 Bosch TC, McFall-Ngai MJ (2011) Metaorganisms as the new frontier. *Zoology* 114:185-190
- 488 Bouckaert R, Vaughan TG, Barido-Sottani J, Duchêne S, Fourment M, Gavryushkina A, Heled J, Jones G,  
489 Kühnert D, De Maio N (2019) BEAST 2.5: An advanced software platform for Bayesian evolutionary  
490 analysis. *PLoS computational biology* 15:e1006650
- 491 Bouffaud ML, Poirier MA, Muller D, Moënne-Loccoz Y (2014) Root microbiome relates to plant host evolution  
492 in maize and other *P oaceae*. *Environmental microbiology* 16:2804-14
- 493 Cai L, Zhou G, Tian RM, Tong H, Zhang W, Sun J, Ding W, Wong YH, Xie JY, Qiu JW, Liu S (2017)  
494 Metagenomic analysis reveals a green sulfur bacterium as a potential coral symbiont. *Scientific reports*  
495 7:1-1.

496 Callahan BJ, McMurdie PJ, Rosen MJ, Han AW, Johnson AJA, Holmes SP (2016) DADA2: high-resolution  
497 sample inference from Illumina amplicon data. *Nature methods* 13:581-583

498 Campbell BJ, Yu L, Heidelberg JF, Kirchman DL (2011) Activity of abundant and rare bacteria in a coastal ocean.  
499 *Proceedings of the National Academy of Sciences* 108:12776-12781

500 Caroselli E, Brambilla V, Ricci F, Mattioli G, Levy O, Falini G, Dubinsky Z, Goffredo S (2016) Inferred  
501 calcification rate of a temperate azooxanthellate caryophylliid coral along a wide latitudinal gradient. *Coral*  
502 *Reefs* 35:919-928

503 Ceh J, Kilburn MR, Cliff JB, Raina JB, van Keulen M, Bourne DG (2013a) Nutrient cycling in early coral life  
504 stages: *Pocillopora damicornis* larvae provide their algal symbiont (*Symbiodinium*) with nitrogen acquired  
505 from bacterial associates. *Ecology and Evolution* 3:2393-2400

506 Ceh J, van Keulen M, Bourne DG (2013b) Intergenerational transfer of specific bacteria in corals and possible  
507 implications for offspring fitness. *Microbial ecology* 65:227-231

508 Chan WY, Peplow LM, Menéndez P, Hoffmann AA, van Oppen MJ (2019). The roles of age, parentage and  
509 environment on bacterial and algal endosymbiont communities in *Acropora* corals. *Molecular Ecology*  
510 28:830-843

511 Chen YH, Yang SH, Tandon K, Lu CY, Chen HJ, Shih CJ, Tang SL (2021) Potential syntrophic relationship  
512 between coral-associated *Prosthecochloris* and its companion sulfate-reducing bacterium unveiled by  
513 genomic analysis. *Microbial Genomics* 7(5)

514 Damjanovic K, Blackall LL, Peplow LM, van Oppen MJ (2020) Assessment of bacterial community composition  
515 within and among *Acropora loripes* colonies in the wild and in captivity. *Coral Reefs* 39:1245-1255

516 Damjanovic K, Menéndez P, Blackall LL, van Oppen MJ (2019) Early life stages of a common broadcast  
517 spawning coral associated with specific bacterial communities despite lack of internalized bacteria.  
518 *Microbial Ecology*:1-14

519 Davis NM, Proctor DM, Holmes SP, Relman DA, Callahan BJ (2018) Simple statistical identification and removal  
520 of contaminant sequences in marker-gene and metagenomics data. *Microbiome* 6:1-14

521 de Mendiburu F, Yaseen M (2020) *Agricolae: Statistical Procedures for Agricultural Research*

522 Douglas AE, Werren JH (2016) Holes in the hologenome: why host-microbe symbioses are not holobionts. *MBio*  
523 7:e02099-15

524 Dunphy CM, Gouhier TC, Chu ND, Vollmer SV (2019) Structure and stability of the coral microbiome in space  
525 and time. *Scientific reports* 9:1-13

526 Durante MK, Baums IB, Williams DE, Vohsen S, Kemp DW (2019) What drives phenotypic divergence among  
527 coral clonemates of *Acropora palmata*? *Molecular ecology* 28(13), 3208-3224

528 Epstein HE, Torda G, Munday PL, van Oppen MJ (2019) Parental and early life stage environments drive  
529 establishment of bacterial and dinoflagellate communities in a common coral. *The ISME Journal* 13:1635-  
530 1638

531 Fordyce AJ, Ainsworth TD, Leggat W (2021) Light Capture, Skeletal Morphology, and the Biomass of Corals'  
532 Boring Endoliths. *Mosphere* 6:e00060-21.

533 Franzenburg S, Walter J, Künzel S, Wang J, Baines JF, Bosch TC, Fraune S (2013) Distinct antimicrobial peptide  
534 expression determines host species-specific bacterial associations. *Proceedings of the National Academy*  
535 *of Sciences* 110:E3730-E3738

536 Freckleton RP, Jetz W (2009) Space versus phylogeny: disentangling phylogenetic and spatial signals in  
537 comparative data. *Proceedings of the Royal Society B: Biological Sciences* 276:21-30

538 Garrett RG (2013) The 'rgr' package for the R Open Source statistical computing and graphics environment-a tool  
539 to support geochemical data interpretation. *Geochemistry: Exploration, Environment, Analysis* 1:355-78.

540 Griffiths SM, Antwis RE, Lenzi L, Lucaci A, Behringer DC, Butler IV MJ, Preziosi RF (2019) Host genetics and  
541 geography influence microbiome composition in the sponge *Ircinia campana*. *Journal of Animal Ecology*  
542 88:1684-95

543 Guyoneaud R, Mouné S, Eatock C, Bothorel V, Hirschler-Réa A, Willison J, Duran R, Liesack W, Herbert R,  
544 Matheron R, Caumette P (2002) Characterization of three spiral-shaped purple nonsulfur bacteria isolated  
545 from coastal lagoon sediments, saline sulfur springs and microbial mats: emended description of the genus  
546 *Roseospira* and description of *Roseospira marina* sp. nov., *Roseospira navarrensis* sp. nov. and *Roseospira*  
547 *thiosulfatophila* sp. nov. *Archives of microbiology* 178:315-324

548 Henry EA, Devereux R, Maki JS, Gilmour CC, Woese CR, Mandelco L, Schauder R, Remsen CC, Mitchell R  
549 (1994) "Characterization of a new thermophilic sulfate-reducing bacterium." *Archives of Microbiology*  
550 161:62-69

551 Hernandez-Agreda A, Leggat W, Bongaerts P, Ainsworth TD (2016) The microbial signature provides insight  
552 into the mechanistic basis of coral success across reef habitats. *MBio*, 7(4)

553 Hester ER, Barott KL, Nulton J, Vermeij MJ, Rohwer FL (2016). Stable and sporadic symbiotic communities of  
554 coral and algal holobionts. *The ISME Journal* 10:1157-1169

555 Huang D, Roy K (2015) The future of evolutionary diversity in reef corals. *Philosophical Transactions of the*  
556 *Royal Society B: Biological Sciences* 370:20140010

557 Jombart T, Dray S (2010) Adephylo: exploratory analyses for the phylogenetic comparative method.  
558 *Bioinformatics* 26:1-21

559 Jorissen H, Galand PE, Bonnard I, Meiling S, Raviglione D, Meistertzheim AL, Hédouin L, Banaigs B, Payri CE,  
560 Nugues MM (2021) Coral larval settlement preferences linked to crustose coralline algae with distinct  
561 chemical and microbial signatures. *Scientific Reports*. 11:1-1

562 Jost L (2010) The relation between evenness and diversity. *Diversity* 2:207-32.

563 Kantor RS, van Zyl AW, van Hille RP, Thomas BC, Harrison ST, Banfield JF (2015) Bioreactor microbial  
564 ecosystems for thiocyanate and cyanide degradation unravelled with genome-resolved metagenomics.  
565 *Environmental microbiology* 17:4929-41

566 Kemp KM, Westrich JR, Alabady MS, Edwards ML, Lipp EK (2018) Abundance and multilocus sequence  
567 analysis of *Vibrio* bacteria associated with diseased elkhorn coral (*Acropora palmata*) of the Florida Keys.  
568 *Applied and environmental microbiology* 8:e01035-17

569 Kolde R (2012) Pheatmap: pretty heatmaps. R package version 1

570 Lahti L, Shetty S (2018) Introduction to the Microbiome R Package

571 Lawler SN, Kellogg CA, France SC, Clostio RW, Brooke SD, Ross SW (2016) Coral-associated bacterial  
572 diversity is conserved across two deep-sea *Anthothela* species. *Frontiers in microbiology* 7:458

573 Legendre P, Borcard D, Peres-Neto PR (2005) Analyzing beta diversity: partitioning the spatial variation of  
574 community composition data. *Ecological monographs* 75:435-450

575 Legendre P, Gallagher ED (2001) Ecologically meaningful transformations for ordination of species data.  
576 *Oecologia* 129:271-280

577 Leite DC, Leão P, Garrido AG, Lins U, Santos HF, Pires DO, Castro CB, van Elsas JD, Zilberberg C, Rosado AS,  
578 Peixoto RS (2017) Broadcast spawning coral *Mussismilia hispida* can vertically transfer its associated  
579 bacterial core. *Frontiers in microbiology* 8:176

580 Leschine SU, Paster BJ, Canale-Parola ER (2006) Free-living saccharolytic spirochetes: the genus *Spirochaeta*.  
581 *The prokaryotes* 7:195-210

582 Lesser M, Stat M, Gates R (2013) The endosymbiotic dinoflagellates (*Symbiodinium* sp.) of corals are parasites  
583 and mutualists. *Coral Reefs* 32:603-611

584 Li G, Zeng X, Liu X, Zhang X, Shao Z (2016) *Wukongibacter baidiensis* gen. nov., sp. nov., an anaerobic  
585 bacterium isolated from hydrothermal sulfides and proposal for the reclassification of the closely related  
586 *Clostridium halophilum* and *Clostridium caminithermale* within *Maledivibacter* gen. nov. and  
587 *Paramaledivibacter* gen. nov., respectively. International journal of systematic and evolutionary  
588 microbiology 66:4355-4361

589 Lim SJ, Bordenstein SR (2020) An introduction to phylosymbiosis. Proceedings of the Royal Society B 287:  
590 20192900

591 Louca S, Polz MF, Mazel F, Albright MB, Huber JA, O'Connor MI, Ackermann M, Hahn AS, Srivastava DS,  
592 Crowe SA (2018) Function and functional redundancy in microbial systems. Nat Ecol Evol 1:936–43

593 Madin JS anderson KD andreasen MH, Bridge TC, Cairns SD, Connolly SR, Darling ES, Diaz M, Falster DS,  
594 Franklin EC, Gates RD (2016) The Coral Trait Database, a curated database of trait information for coral  
595 species from the global oceans. Scientific Data, 3(1), pp.1-22

596 Magnusson SH, Fine M, Kühl M. (2007) Light microclimate of endolithic phototrophs in the scleractinian corals  
597 *Montipora monasteriata* and *Porites cylindrica*. Marine Ecol Prog Ser. 332:119–28.

598 Maher RL, Rice MM, McMinds R, Burkepile DE, Thurber RV (2019) Multiple stressors interact primarily  
599 through antagonism to drive changes in the coral microbiome. Scientific reports 9:1-12

600 Marcelino VR, Morrow KM, van Oppen MJ, Bourne DG, Verbruggen H (2017) Diversity and stability of coral  
601 endolithic microbial communities at a naturally high pCO<sub>2</sub> reef. Molecular Ecology 26:5344-5357

602 Marcelino VR, Verbruggen H (2016) Multi-marker metabarcoding of coral skeletons reveals a rich microbiome  
603 and diverse evolutionary origins of endolithic algae. Sci Rep 6:31508

604 Marcelino LA, Westneat MW, Stoyneva V, Henss J, Rogers JD, Radosevich A, Turzhitsky V, Siple M, Fang A,  
605 Swain TD (2013) Modulation of light-enhancement to symbiotic algae by light-scattering in corals and  
606 evolutionary trends in bleaching. PLoS One 8:e61492

607 Martin M (2011) Cutadapt removes adapter sequences from high-throughput sequencing reads. EMBnet journal  
608 17:10-12

609 Massé A, Domart-Coulon I, Golubic S, Duché D, Tribollet A (2018) Early skeletal colonization of the coral  
610 holobiont by the microboring Ulvophyceae *Ostreobium* sp. Scientific reports. 8:1-1.

611 Mazel F, Davis KM, Loudon A, Kwong WK, Groussin M, Parfrey LW (2018) Is host filtering the main driver of  
612 phylosymbiosis across the tree of life? Msystems 3:e00097-18

613 McDevitt-Irwin JM, Baum JK, Garren M, Vega Thurber RL (2017) Responses of coral-associated bacterial  
614 communities to local and global stressors. *Frontiers in Marine Science*. 4:262

615 McMurdie PJ, Holmes S (2013) phyloseq: an R package for reproducible interactive analysis and graphics of  
616 microbiome census data. *PloS one* 8:e61217

617 Neave MJ, Rachmawati R, Xun L, Michell CT, Bourne DG, Apprill A, Voolstra CR (2017) Differential specificity  
618 between closely related corals and abundant *Endozoicomonas* endosymbionts across global scales. *The*  
619 *ISME journal*. 11:186-200

620 Neave MJ, Apprill A, Ferrier-Pagès C, Voolstra CR (2016) Diversity and function of prevalent symbiotic marine  
621 bacteria in the genus *Endozoicomonas*. *Applied microbiology and biotechnology* 100(19), 8315-8324

622 Nitschke MR, Davy SK, Ward S (2016) Horizontal transmission of Symbiodinium cells between adult and  
623 juvenile corals is aided by benthic sediment. *Coral Reefs* 35:335-344

624 Ofek M, Hadar Y, Minz D (2012) Ecology of root colonizing *Massilia* (Oxalobacteraceae). *PloS one* 7:40117

625 Otsu N (1979) A threshold selection method from gray-level histograms. *IEEE transactions on systems, man and*  
626 *cybernetics* 9:62-66

627 O'Brien PA, Tan S, Yang C, Frade PR andreakis N, Smith HA, Miller DJ, Webster NS, Zhang G, Bourne DG  
628 (2020) Diverse coral reef invertebrates exhibit patterns of phylosymbiosis. *The ISME journal* 14:2211-  
629 2222

630 Paradis E, Schliep K (2019) "ape 5.0: an environment for modern phylogenetics and evolutionary analyses in R.". *Bioinformatics*:526-528

631

632 Patton JS, Abraham S, Benson AA (1977) Lipogenesis in the intact coral *Pocillopora capitata* and its isolated  
633 zooxanthellae: evidence for a light-driven carbon cycle between symbiont and host. *Marine Biology*  
634 44:235-247

635 Peixoto RS, Sweet M, Villela HD, Cardoso P, Thomas T, Voolstra CR, Høj L, Bourne DG (2021) Coral probiotics:  
636 premise, promise, prospects. *Annual review of animal biosciences* 9:265-88

637 Pollock FJ, McMinds R, Smith S, Bourne DG, Willis BL, Medina M, Thurber RV, Zaneveld JR (2018) Coral-  
638 associated bacteria demonstrate phylosymbiosis and cophylogeny. *Nature Communications* 9:4921

639 Pinnaka AK, Tanuku NRS (2014) *The family Cyclobacteriaceae*. Berlin: Springer-Verlag

640 Quast C, Priesse E, Yilmaz P, Gerken J, Schweer T, Yarza P, Peplies J, Glöckner FO (2012) The SILVA  
641 ribosomal RNA gene database project: improved data processing and web-based tools. *Nucleic acids*  
642 *research* 41:D590-D596

643 Quigley KM, Warner PA, Bay LK, Willis BL (2018) Unexpected mixed-mode transmission and moderate genetic  
644 regulation of *Symbiodinium* communities in a brooding coral. *Heredity* 121:524-536

645 Ralph PJ, Larkum AWD, Kühl M (2007) Photobiology of endolithic microorganisms in living coral skeletons: 1.  
646 Pigmentation, spectral reflectance and variable chlorophyll fluorescence analysis of endoliths in the  
647 massive corals *Cyphastrea serailia*, *Porites lutea* and *Goniastrea australensis*. *Marine Biology* 152.2: 395-  
648 404

649 Ricci F, Fordyce A, Leggat W, Blackall LL, Ainsworth T, Verbruggen H (2021) Multiple techniques point to  
650 oxygenic phototrophs dominating the *Isopora palifera* skeletal microbiome. *Coral Reefs*:1-8

651 Ricci F, Marcelino VR, Blackall LL, Kühl M, Medina M, Verbruggen H (2019) Beneath the surface: community  
652 assembly and functions of the coral skeleton microbiome. *Microbiome* 7:159

653 Rosales SM, Miller MW, Williams DE, Traylor-Knowles N, Young B, Serrano XM (2019) Microbiome  
654 differences in disease-resistant vs. susceptible *Acropora* corals subjected to disease challenge assays.  
655 *Scientific reports* 9:1-11

656 Rosenberg E, Zilber-Rosenberg I (2018) The hologenome concept of evolution after 10 years. *Microbiome* 6:1-  
657 14

658 Rosenberg E, Sharon G, Zilber-Rosenberg I (2009) The hologenome theory of evolution contains Lamarckian  
659 aspects within a Darwinian framework. *Environ Microbiol* 11:2959-2962

660 Ryan RP, Monchy S, Cardinale M, Taghavi S, Crossman L, Avison MB, Berg G, Van Der Lelie D, Dow JM  
661 (2009) The versatility and adaptation of bacteria from the genus *Stenotrophomonas*. *Nature Reviews*  
662 *Microbiology* 7:514-525

663 Schmitz-Esser S, Tischler P, Arnold R, Montanaro J, Wagner M, Rattei T, Horn M (2010). The genome of the  
664 amoeba symbiont “*Candidatus* Amoebophilus asiaticus” reveals common mechanisms for host cell  
665 interaction among amoeba-associated bacteria. *Journal of Bacteriology* 192:1045-1057

666 Segata N, Izard J, Waldron L, Gevers D, Miropolsky L, Garrett WS, Huttenhower C (2011) Metagenomic  
667 biomarker discovery and explanation. *Genome biology* 12:1-18

668 Shnit-Orland M, Sivan A, Kushmaro A (2012) Antibacterial activity of *Pseudoalteromonas* in the coral holobiont.  
669 *Microbial ecology* 64:851-859

670 Simpson G (2015) ggvegan: ‘ggplot2’ Plots for the ‘vegan’ Package. R Package Version 00–3

671 Su Y, Zhou Z, Yu X (2018) Possible roles of glutamine synthetase in responding to environmental changes in a  
672 scleractinian coral. *Molecular biology reports* 45:2115-2124

673 Tandon K, Lu CY, Chiang PW, Wada N, Yang SH, Chan YF, Chen PY, Chang HY, Chiou YJ, Chou MS, Chen  
674 WM (2020) Comparative genomics: Dominant coral-bacterium *Endozoicomonas acroporae* metabolizes  
675 dimethylsulfoniopropionate (DMS). The ISME Journal 14:1290-1303

676 Tang Y, Horikoshi M, Li W (2016) ggfortify: Unified interface to visualize statistical results of popular R  
677 packages. R J 8:474

678 Ter Braak CJ (1987) The analysis of vegetation-environment relationships by canonical correspondence analysis.  
679 Vegetatio 69:69-77

680 Venables WN, Ripley BD (2002) MASS (R package). Modern Applied Statistics with S software

681 Woolstra CR, Ziegler M (2020) Adapting with microbial help: microbiome flexibility facilitates rapid responses  
682 to environmental change. BioEssays. 42:2000004.

683 Wang W, Luo X, Ye X, Chen Y, Wang H, Wang L, Wang Y, Yang Y, Li Z, Cao H, Cui Z (2020a) Predatory  
684 Myxococcales are widely distributed in and closely correlated with the bacterial community structure of  
685 agricultural land. Applied Soil Ecology 146:103365

686 Wang S, Meade A, Lam HM, Luo H (2020b) Evolutionary timeline and genomic plasticity underlying the lifestyle  
687 diversity in Rhizobiales. Msystems 5:e00438-20

688 Wickham H (2015) R packages: organize, test, document, and share your code. " O'Reilly Media, Inc."

689 Wickham H (2011) ggplot2. Wiley Interdisciplinary Reviews: Computational Statistics 3:180-185

690 Williams AD, Brown BE, Putschim L, Sweet MJ (2015) Age-related shifts in bacterial diversity in a reef coral.  
691 PLoS One 10:e0144902

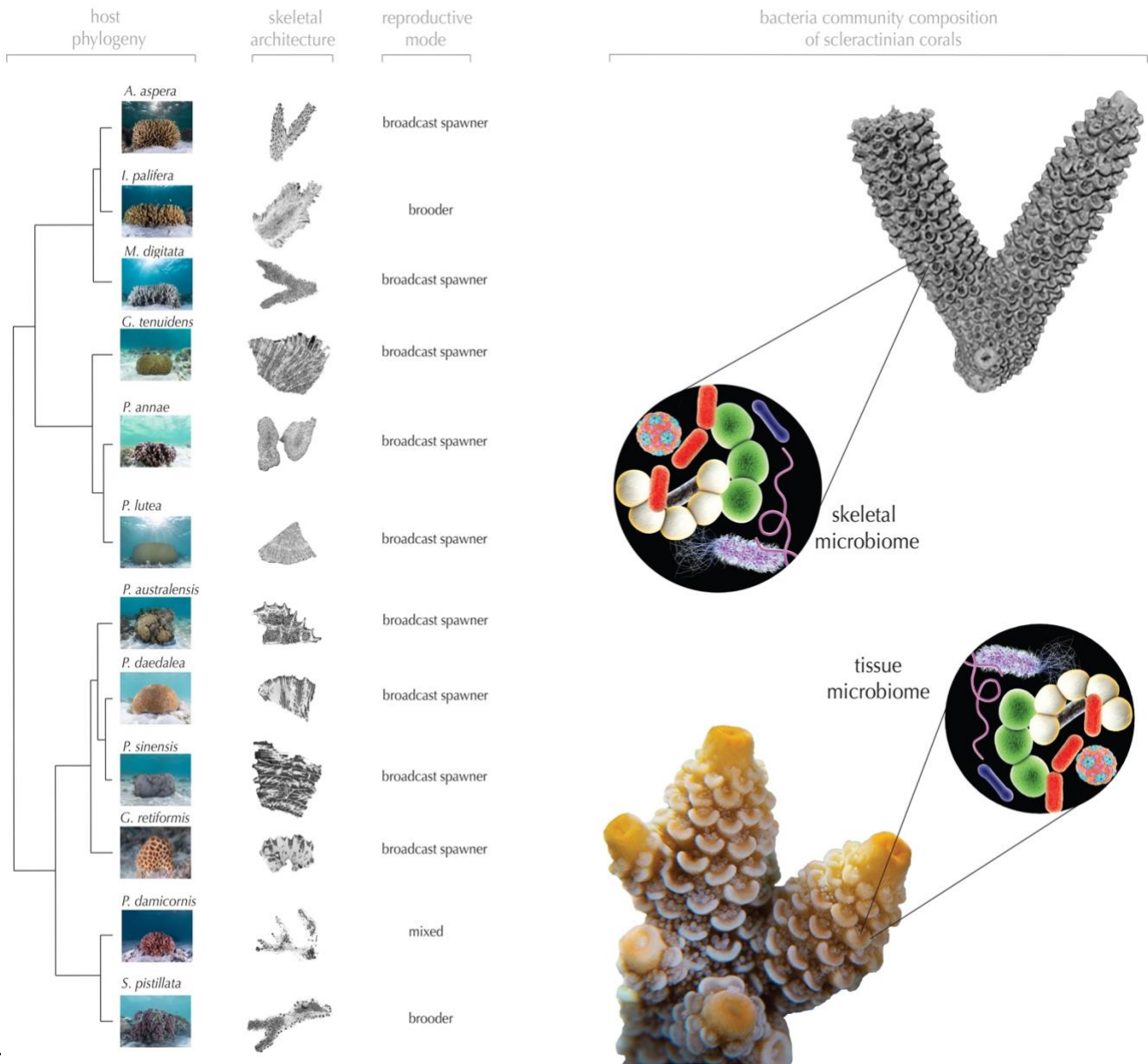
692 Yang Cao (2020) microbiomeMarker: microbiome biomarker analysis. R package version 0.0.1.9000.  
693 <https://github.com/yiluheihei/microbiomeMarker>. DOI: 10.5281/zenodo.3749415.

694 Zilber-Rosenberg I, Rosenberg E (2008) Role of microorganisms in the evolution of animals and plants: the  
695 hologenome theory of evolution. FEMS Microbiol Rev 32:723-735

696 Zhou G, Cai L, Yuan T, Tian R, Tong H, Zhang W, Jiang L, Guo M, Liu S, Qian PY, Huang H (2017) Microbiome  
697 dynamics in early life stages of the scleractinian coral *Acropora gemmifera* in response to elevated pCO<sub>2</sub>.  
698 Environmental microbiology 19:3342-3352

699  
700  
701  
702

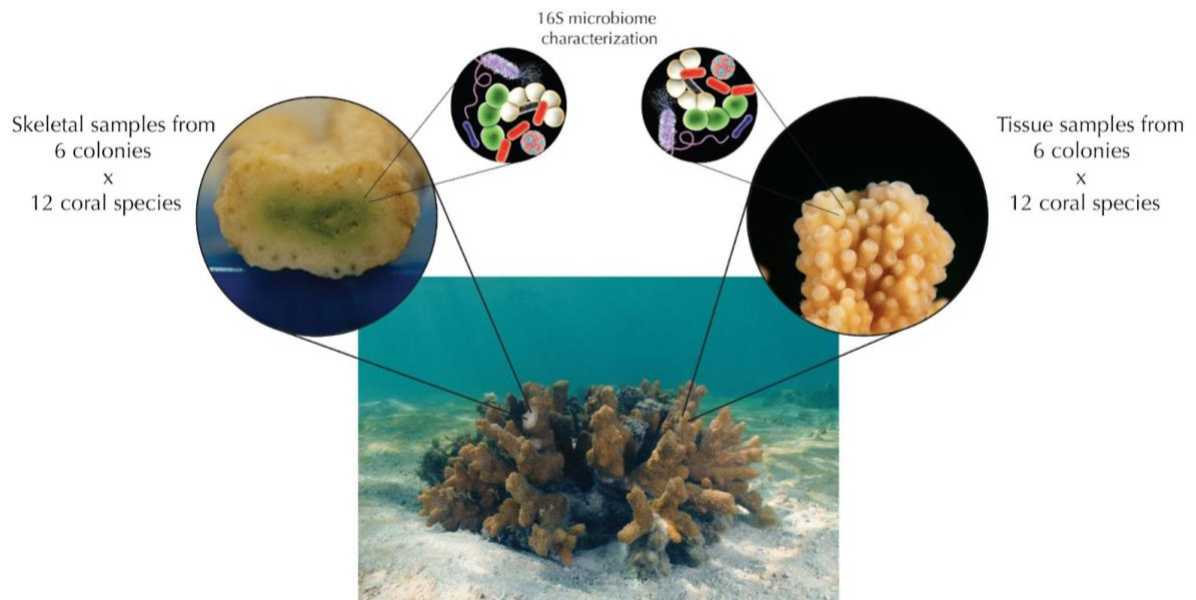
704



706  
707

708 **Figure 1.** Vignette of the experimental design aiming to answer the question: to which extent host  
709 phylogeny, skeletal architecture and reproductive mode affect the microbiome composition of tissue  
710 and skeleton of scleractinian corals?

711  
712



713

714 **Figure 2.** Vignette of the experimental design aiming to answer the questions: what are the microbiome  
715 structure of tissue and skeleton of scleractinian corals and how do they differ?

716

717

718

719

720

721

722

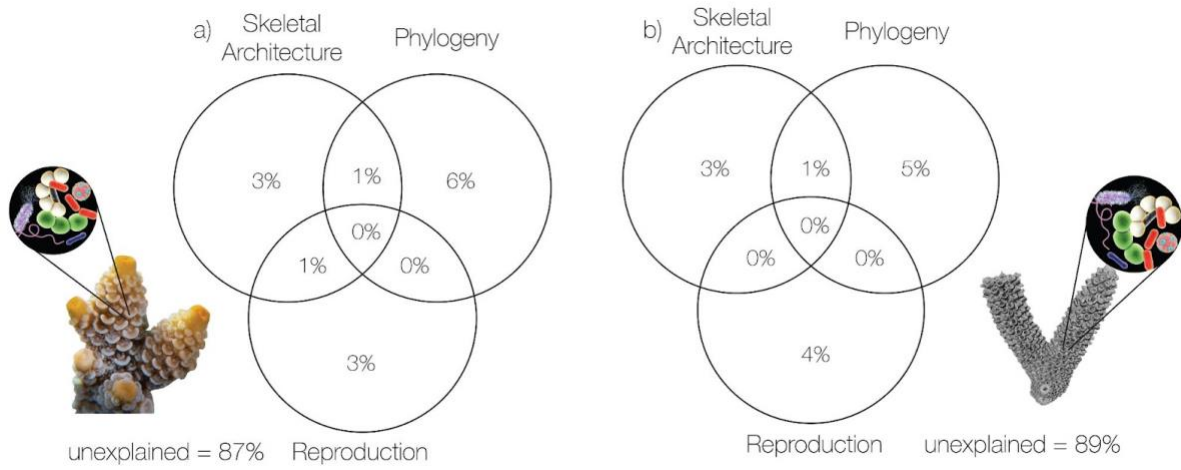
723

724

725

726

727



728

729 **Figure 3.** Partitioning the variation in bacterial communities composition of coral tissue (a) and  
 730 skeleton (b) explained by host skeletal architecture, phylogeny, and reproductive mode. Adjusted  $R^2$  are  
 731 given.

732

733

734

735

736

737

738

739

740

741

742

743

744

745

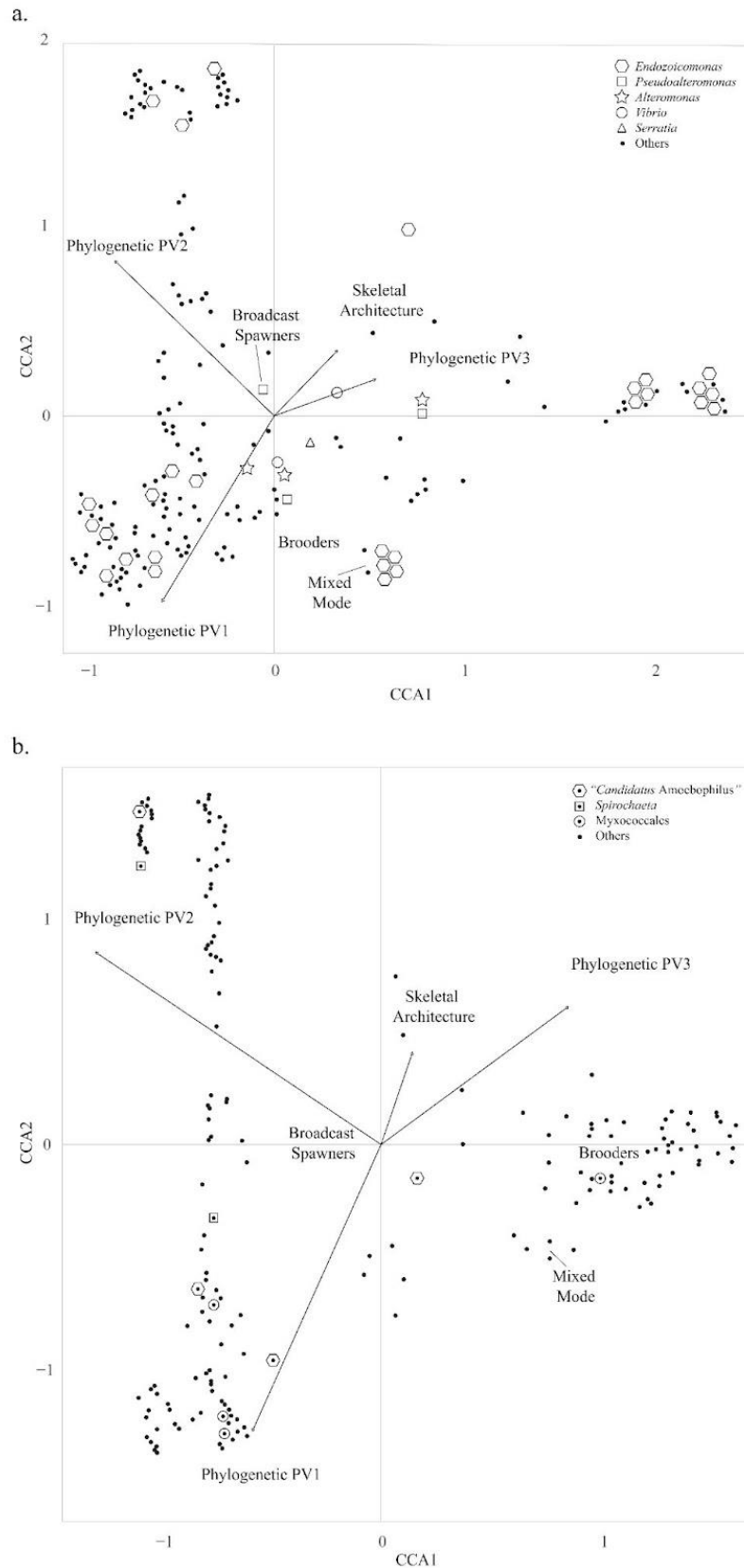
746

747

748

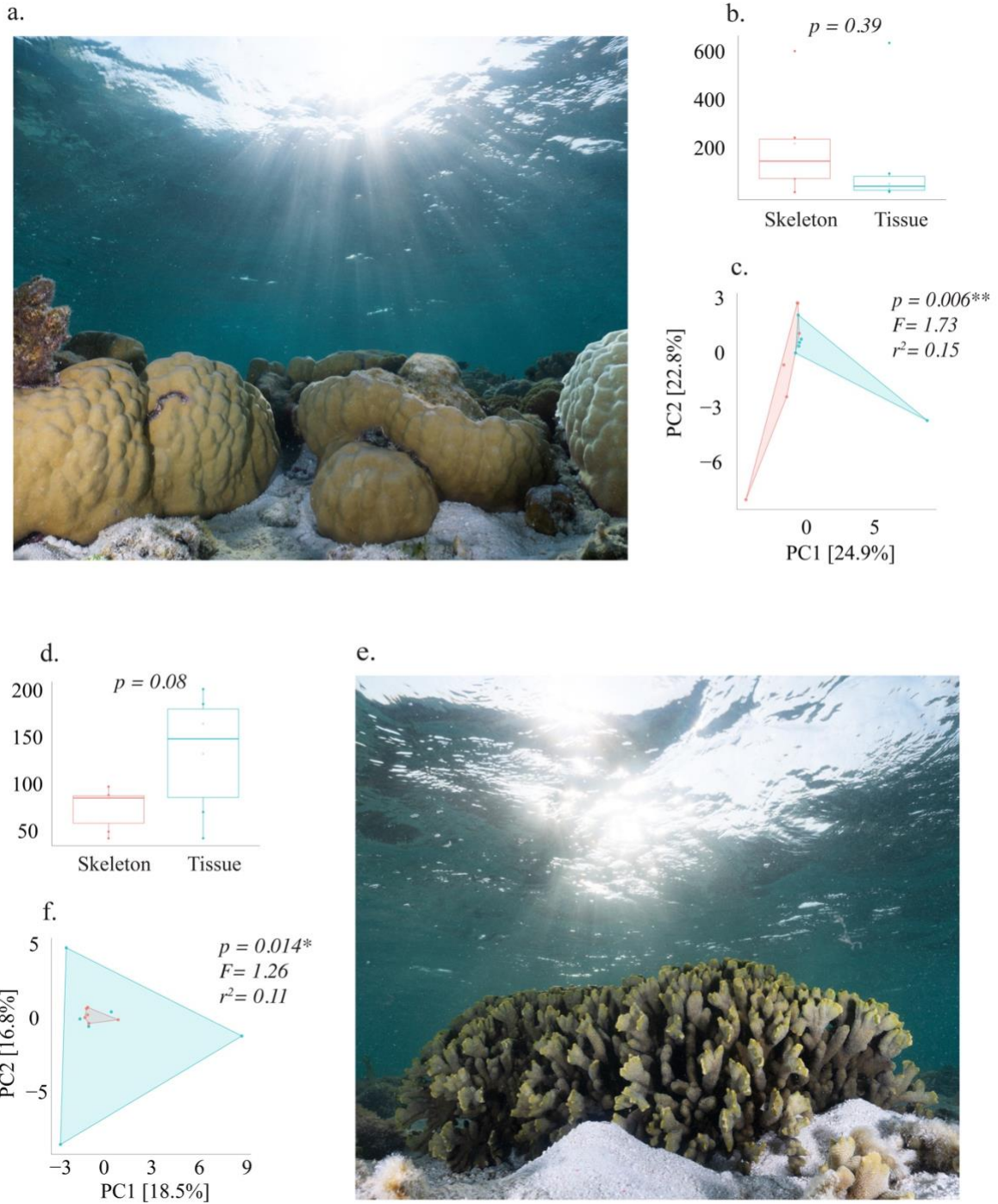
749

750



751

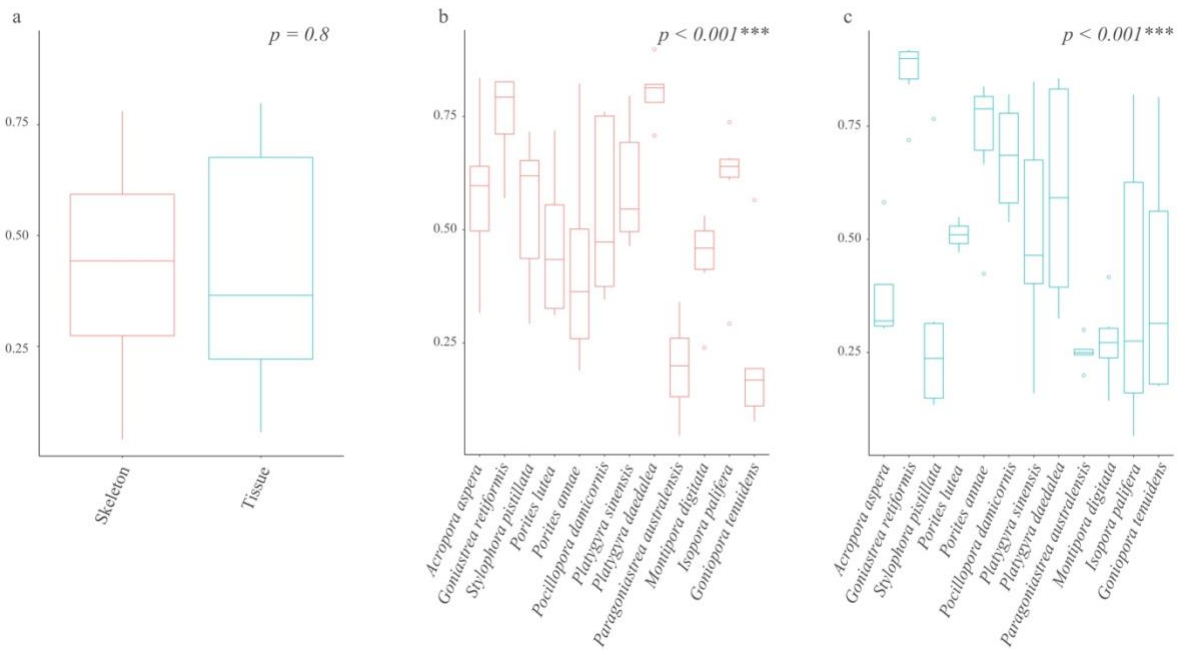
752 **Figure 4.** CCA biplot representing the tissue (a) and skeletal (b) microbiome structure according to each  
 753 explanatory variable. Arrows represent quantitative explanatory variables Skeletal Architecture, Phylogeny PV1,  
 754 2, and 3, with arrowheads indicating direction of increase. Categorical explanatory variables Broadcast Spawners,  
 755 Brooders, and Mixed Mode are positioned on the biplot according to their coordinates. All the explanatory  
 756 variables in both cca biplots were highly significant ( $p < 0.001$ ).



757  
 758  
 759  
 760  
 761  
 762  
 763  
 764  
 765  
 766  
 767

**Figure 5.** Plots showing differences in microbial communities of *Porites lutea* (a-c), and *Montipora digitata* (d-f). Box-plots b and e show comparisons between observed richness (α-diversity) of tissue and skeleton microbial communities. PCA plots c and f show comparison between tissue (blue) and skeletal (red) microbiome composition and NPMANOVA results. Refer to Supplementary Figure 3 and 4 for additional coral species.





774

775 **Supplementary Figure 2.** Boxplots showing Pielou evenness indexes of the skeleton (red) and tissue  
 776 (blue) of scleractinian corals (a) and each coral species (b and c). Within each plot are reported the  $p$ -  
 777 value calculated by means of Mann-Whitney U Test (a), Analysis of Variance (b) and Kruskal–Wallis  
 778 test (c).

779

780

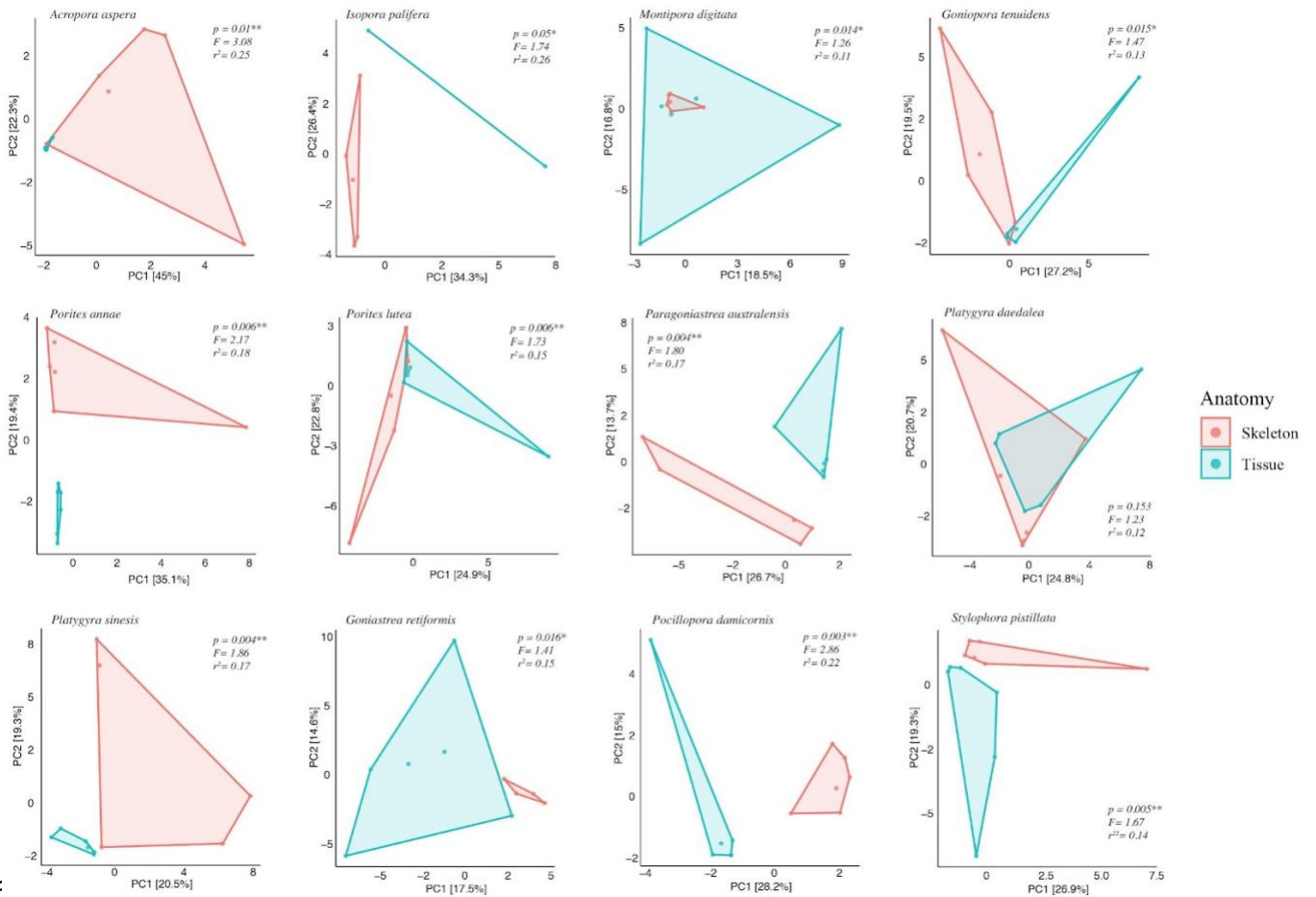
781

782

783

784

785

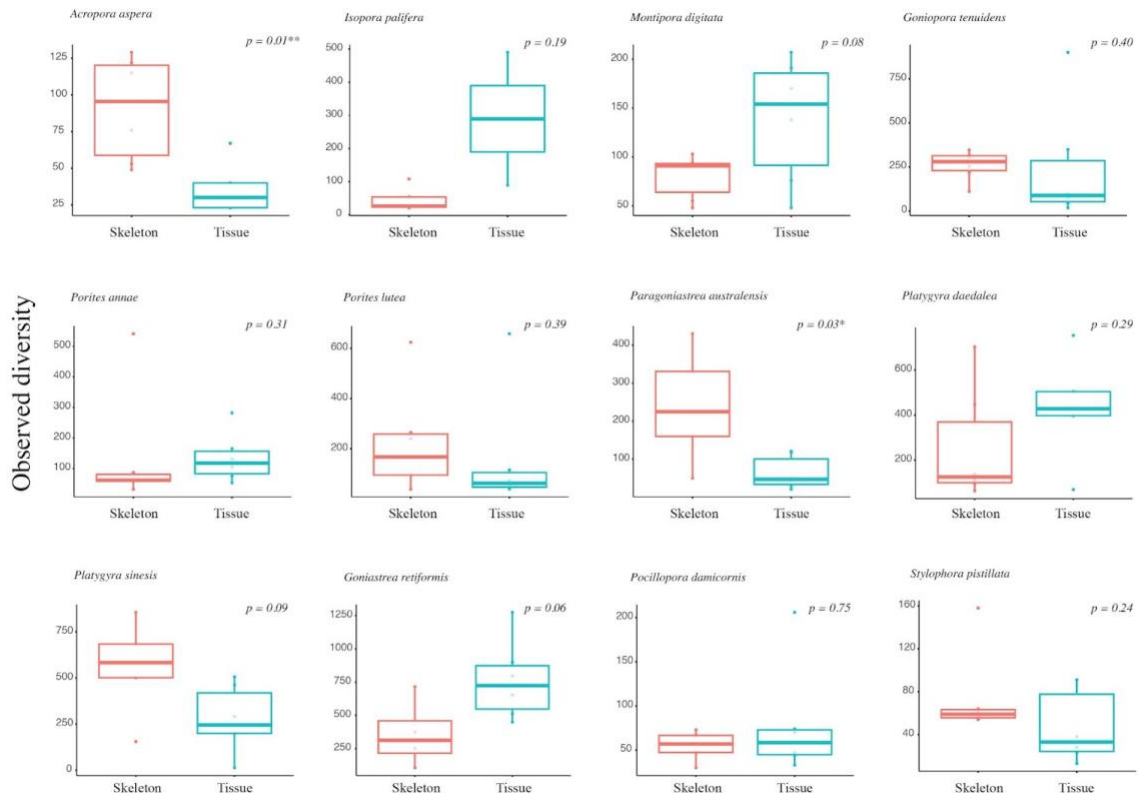


786

787

788 **Supplementary Figure 3.** Biplots showing PCA of each coral species. Red dots and areas represent  
 789 skeletal samples, while blue areas and samples represent tissue samples. Within each biplot are also  
 790 reported the results of NPMANOVA analyses assessing differences in composition between the  
 791 prokaryotic communities of skeleton and tissue of each coral species.

792



793

794 **Supplementary Figure 4.** Boxplots showing observed  $\alpha$ -diversity measures of the tissue (blue) and  
 795 skeleton (red) of each coral species. Within each plot are reported the  $p$ -value calculated by means of  
 796 Welsh T-test or Mann-Whitney U Test.

797

798

799

800

801

802

803

804

805

806

807

808

809

810

811

812

813

814

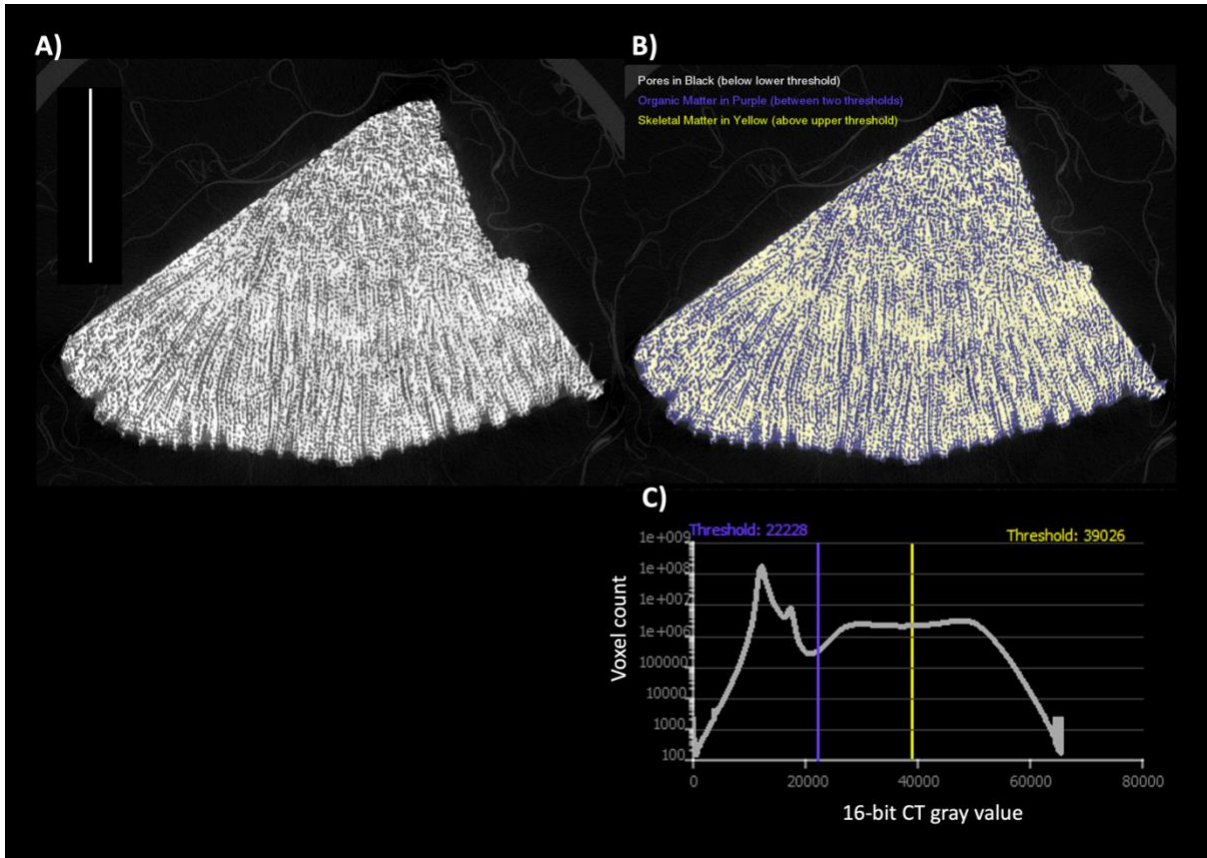
815

816

817

818

819

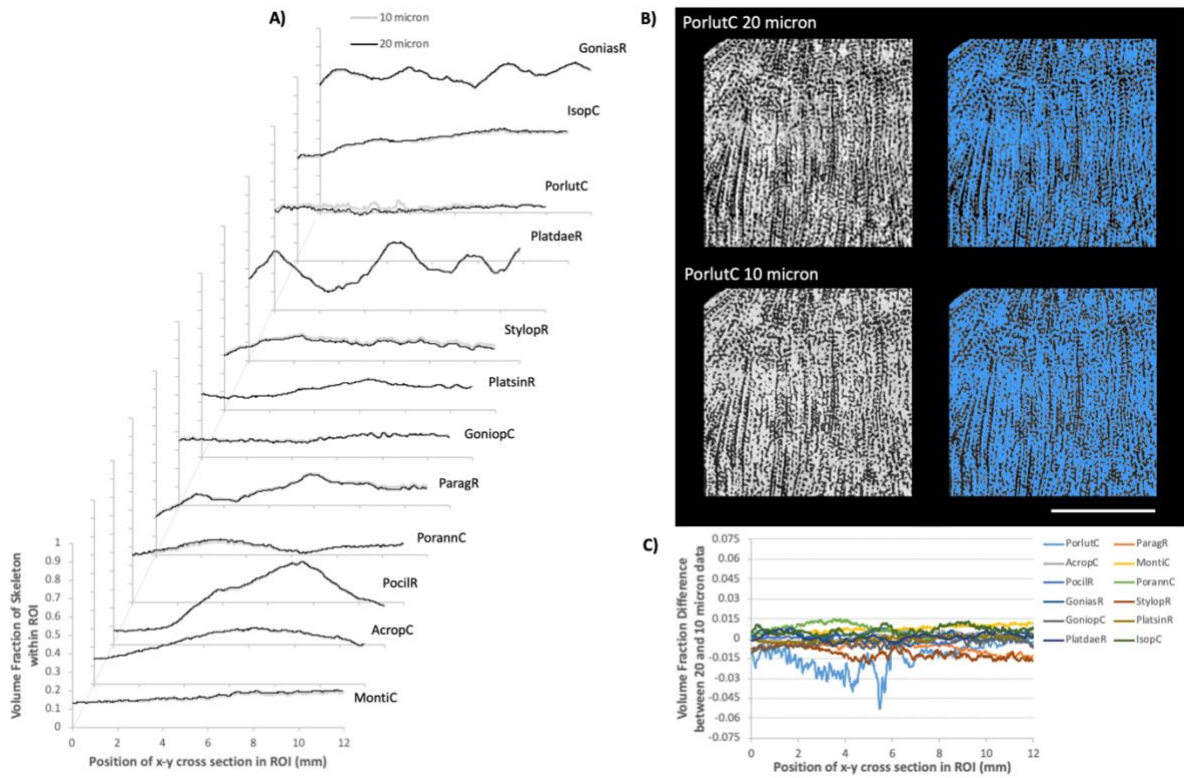


820

821 **Supplementary Figure 5.** (a) Representative slice of micro-CT data through a sample of *Porites lutea*  
 822 (FRH49) showing denser structure as brighter gray to white values and less dense structure, such as air,  
 823 as dark gray to black values surrounding the specimen. (b) Same slice segmented into 3 phases: skeletal  
 824 material (shaded yellow); organic matrix (shaded purple); and air/bubble wrap within and surrounding  
 825 the specimen (unshaded gray values). (c) Grayscale histogram of 16-bit micro-CT data showing the  
 826 points of segmentation between the different phases. The two peaks within the lowest density phase  
 827 represent the air within and surrounding the specimen (peak around 12000) and bubble wrap and plastic  
 828 specimen holder (peak around 17000). The white bar in part A is a 10 mm scale bar.

829

830



832  
833  
834

835 **Supplementary Figure 6.** (a) Plots of skeletal volume trends within the x-y cross section of a 12x12x12  
836 mm<sup>3</sup> ROI as function of distance along the z-axis of the ROI for both 20 micrometer and 10 micrometer  
837 micro-CT data. (b) Representative slice (at 4.3 mm) from sample PorlutC comparing the 20 micrometer  
838 to 10 micrometer micro-CT data (left hand figures) and segmented skeleton in both (right hand figures).  
839 White scale bar = 6mm. (c) Difference between the 20 micrometer and 10 micrometer data trends  
840 plotted in part A highlighting the very small variability within the porosity trends with no consistent  
841 trend towards an under- or over- estimate of porosity at one given resolution.

842  
843  
844

845  
846

847  
848  
849  
850  
851  
852  
853

854  
855  
856



## Supplementary Files

This is a list of supplementary files associated with this preprint. Click to download.

- [SuppData1LeFSe.xlsx](#)
- [SuppData2coremicrobiome.xlsx](#)
- [SuppData3speciescoremicrobiome.xlsx](#)
- [SuppData4n2fixsulfred.xlsx](#)
- [SuppData5Xcoralenvironment.xlsx](#)